ELSEVIER

Surface Science 507–510 (2002) 560–566

SURFACE SCIENCE

www.elsevier.com/locate/susc

Growth of Fe-based spin aligners on semiconducting substrates

F. Zavaliche *, M. Przybylski [1], W. Wulfhekel, J. Grabowski, R. Scholz, J. Kirschner

Max-Planck-Institut für Mikrostrukturphysik, Weinberg 2, D-06120 Halle, Germany

Abstract

We report on the magnetic and structural characterization of Au/(Ni)Fe/MgO/Fe magneto-tunnel junctions grown on InP(0 0 1) and GaAs(0 0 1). On GaAs substrates almost perfect single crystal junctions with sharp interfaces were achieved as seen by low energy electron diffraction and transmission electron microscopy. In situ magnetization loops obtained with the longitudinal magneto-optic Kerr effect show an independent switching of magnetization of both Fe layers suggesting that the two Fe layers are magnetically decoupled by the MgO layer.

Keywords: Growth; Iron; Semiconducting surfaces; Metallic films; Magnetic measurements

1. Introduction

The potential use of the electron spin in semiconductor based electronic circuits leads to an increased interest in the growth of epitaxial ferromagnetic metal films (FM) on semiconductor substrates (SC) [1]. The idea is based on the spin-polarized transport from the FM spin aligner into the SC element where the spin information is processed. A high spin polarization of the electrons injected into semiconductor was obtained lately using magnetic semiconductors (of almost 100% polarization and comparable resistivity) as a spin aligner. However, these results were obtained at large external magnetic fields and low temperatures [2]. For technical applications, metal-based FM spin aligners, which operate at weak magnetic fields and room temperature (RT), still remain a subject of great interest. Unfortunately, the experiments on spin injection across the metal–FM/SC interface performed so far, have only shown effects of less than 1–2% [3], in agreement with the theoretical predictions for diffusive electron transport. In this case, the net resistance of the circuit is dominated by the resistance of the semiconductor that is spin independent [4]. A number of ideas to circumvent the resistivity mismatch were considered [5–7]. Recent theoretical works predict that the spin injection efficiency from a FM into a SC can be improved if hot electrons created by tunneling, e.g. through an insulating (I) barrier are used, since such a tunneling process is not affected by the resistance mismatch [5,6]. If one

* Corresponding author. Tel.: +49-345-5582-969; fax: +49-345-5582-566.

E-mail address: mprzybyl@mpi-halle.de (F. Zavaliche).

[1] On leave from: Solid State Physics Department, Faculty of Physics and Nuclear Techniques, University of Mining and Metallurgy, al. Mickiewicza 30, 30-059 Krakow, Poland.

0039-6028/02/$ - see front matter
PII: S0039-6028(02)01309-2

considers that very high spin polarizations can be achieved by the spin filtering effect of hot electrons [8], then a possible solution for spin injection would employ a second FM layer between the I layer and SC. To achieve the desired effect, the thickness of this intermediate FM layer should scale with the inelastic mean free path of spin up or spin down electrons. Even then, the efficiency of the M/I/FM/SC tunnel junctions for spin alignment is limited by the relatively low electron polarization at the Fermi level for the metal ferromagnets. However, if tunneling occurs between two ferromagnets, the spin description of the states available for tunneling comes into play. Effectively, an additional spin dependent barrier is introduced, such that, there is a lower impedance when the two FM layers are magnetically aligned than anti-aligned. In other words, the structure exhibits tunneling magnetoresistance (TMR) which ensures an increased spin polarization [9]. For Fe/MgO/Fe junctions a large effect is predicted theoretically [10], and very recently experimentally confirmed [11].

We report on the characterization of (Ni)/Fe/MgO/Fe multilayers grown on InP(0 0 1) and GaAs(0 0 1), widely used in high speed (opto-) electronic applications. Emphasis is given on the crystallographic quality of the junctions resulting from the good epitaxial growth due to the low lattice mismatch between the substrate and the Fe film, as well as between the subsequent films. The hardening of the top Fe film by covering with Ni is performed in order to realize the independent switching of magnetization in the both FM films.

2. Experiment

Sample preparation and characterization were carried out in an ultrahigh vacuum (UHV) multichamber system equipped with molecular beam epitaxy (MBE), Auger electron spectroscopy (AES), low energy electron diffraction (LEED), scanning tunneling microscopy (STM) and in-situ magneto-optic Kerr effect (MOKE). MOKE loops were collected in the longitudinal geometry using an electromagnet with a maximum field of 300 Oe, and an intensity stabilized laser diode (wavelength 670 nm).

The InP and GaAs substrates were cleaned by 500 eV Ar^+ sputtering at elevated temperatures without any prior chemical treatment. Special precaution was taken to avoid approaching the substrate decomposition temperatures (about 600 and 900 K for InP and GaAs, respectively) in order to prevent In and Ga droplet formation. After the cleaning procedures were completed, no traces of contamination were detected in the AES spectra and sharp LEED patterns were observed. Fe, Ni, MgO and Au were deposited at a rate of 1–1.5 ML/min. by electron beam evaporation from thoroughly outgassed high-purity iron, nickel and MgO rods, as well as from a Mo crucible in the case of Au. The growth was carried out at RT at a pressure below 8×10^{-10} mbar.

3. Results and discussion

3.1. Magnetically "alive" Fe films grown on InP(0 0 1) and GaAs(0 0 1)

In the case of Fe grown on P-rich (2×4) InP(0 0 1), the formation of magnetically dead layers at the interface was suppressed by the preparation of InP(0 0 1) surface by sputtering with low energy Ar ions at a temperature 590 K. In addition, a reduced intermixing with the substrate constituents was also clearly confirmed by a detailed AES analysis [12]. The onset of magnetization at RT was detected at an Fe film thickness slightly below 4 ML. Further AES spectra show a small amount of In floating on the top of Fe film, which might be responsible for the observed lack of any LEED pattern. The STM image of a 14 ML thick Fe film (Fig. 1a) shows small islands, with maximum height is about 3 ML as one can see from the corresponding line profile.

A similar procedure of surface preparation was applied for GaAs(0 0 1). However, a sputtering temperature close to 860 K was required to obtain a Ga terminated (4×6)-like reconstruction, which is found to protect the Fe film against strong intermixing with As and Ga. MOKE data show that already a 2 ML thick Fe layer is magnetically

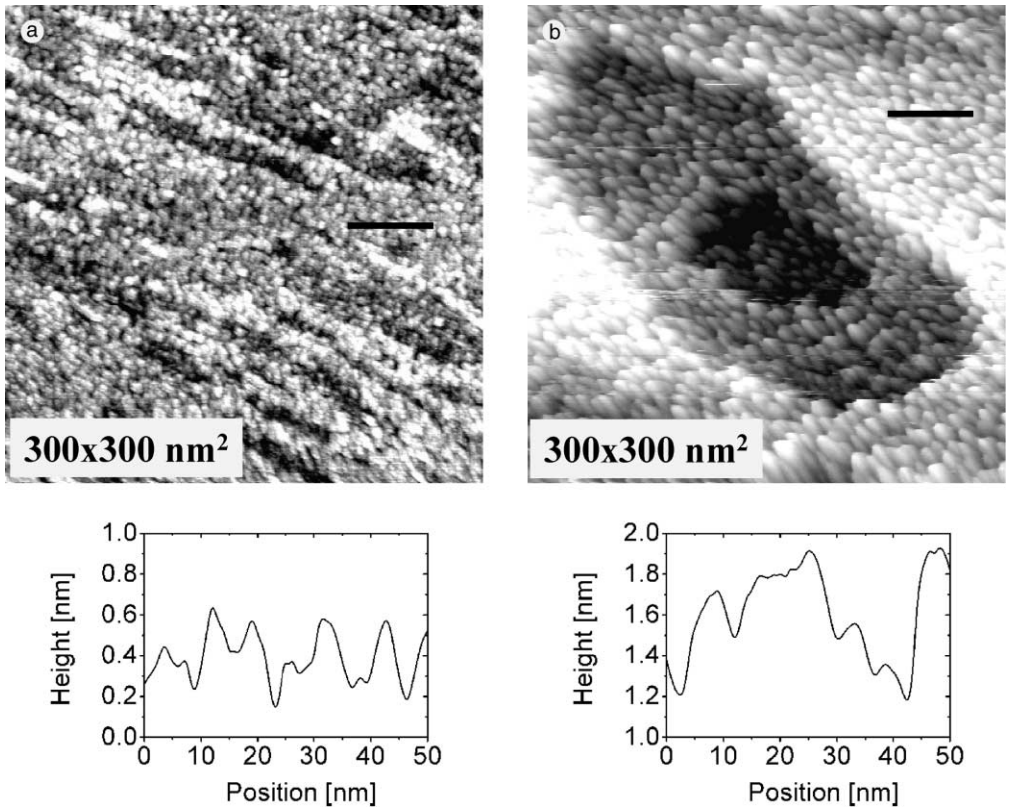

Fig. 1. STM images of about 14 ML of Fe deposited at RT: (a) on InP(0 0 1), and (b) on GaAs(0 0 1). The scans were taken at 1.4 V, 0.2 nA in (a), and −1.0 V, 0.1 nA in (b). The line profiles were taken along the lines shown in the corresponding STM scans.

"alive", however showing a superparamagnetic behavior caused by the island growth of Fe on GaAs(0 0 1) in the initial stage [13]. Ferromagnetism sets in at RT for an Fe thickness of less than 3 ML. The behavior of the ellipticity at remanence vs. the film thickness confirms that vanishing magnetically dead layers form at the Fe/GaAs (0 0 1) interface [13,14]. However, annealing of Fe/GaAs(0 0 1) above 400 K enhances interdiffusion and suppresses the ferromagnetic order in the Fe films. A maximum island height of about 5 ML was observed by STM for a 14 ML thick Fe film grown at RT (Fig. 1b). A reduction of the film roughness by preparation at elevated temperatures is not feasible due to intermixing.

In spite of the Fe films roughness, by a proper choice of the low energy Ar^+ sputtering temperature, we were able to avoid the formation of magnetically dead layers in the RT grown Fe films, both on InP(0 0 1) and GaAs(0 0 1).

3.2. Magnetic anisotropy in Fe films grown on InP(0 0 1) and GaAs(0 0 1)

For both substrates, the Fe films are magnetized in plane. This is because the total anisotropy energy balance of the Fe/SC interface anisotropy and the shape anisotropy favors the magnetization to lie in the film plane. In the case of Fe grown on InP(0 0 1), the films show an uniaxial in-plane magnetic anisotropy with the easy-axis along $[\bar{1}\,1\,0]$ up to a thickness of about 13–15 ML [12]. We found a very similar behavior for Fe grown on GaAs(0 0 1), which shows a dominant uniaxial contribution to the in-plane anisotropy with the easy-axis along the $[\bar{1}\,1\,0]$ direction in the thickness

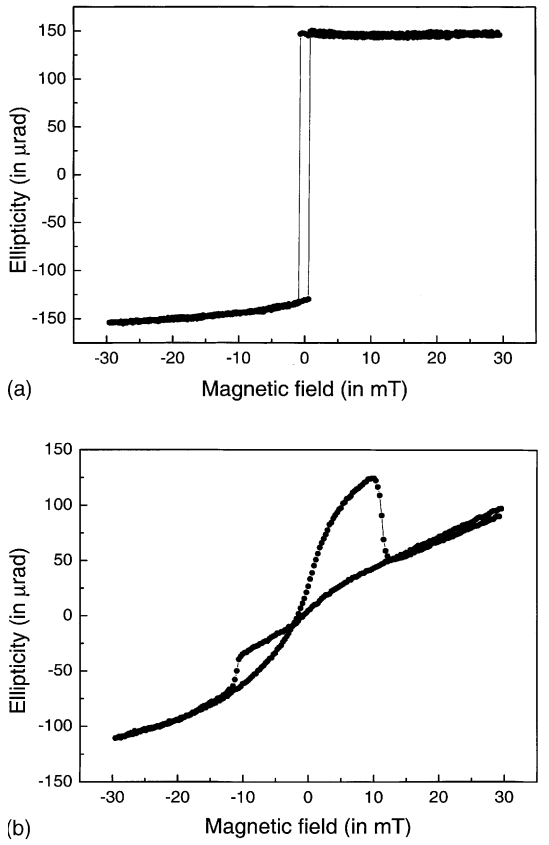

Fig. 2. MOKE loops measured at RT for 14 ML of Fe deposited on GaAs(0 0 1): (a) along the substrate [$\bar{1}$ 1 0] direction (easy-axis of magnetization), (b) along the substrate [1 1 0] direction (hard-axis of magnetization).

range up to about 20 ML (Fig. 2a). However, our MOKE measurements performed along the hard-axis [1 1 0] direction suggest a complex magnetization process in this case (Fig. 2b). In addition to the uniaxial anisotropy, the bcc-Fe film shows a fourfold crystal anisotropy with easy-axis along [1 0 0] directions, i.e., 45° away from the uniaxial easy-axis. The shape of the loop reflects, in our opinion, that beside the continuous magnetization rotation process, the magnetization jumps to the nearest easy-axis (along [1 0 0], [0 $\bar{1}$ 0] or [0 $\bar{1}$ 0]) closer to the direction of the applied field [15]. Additionally, if the applied field is slightly tilted with respect to the sample [1 1 0] direction, the symmetry is broken and the loops become asymmetric. Forward and backward branches show jumps at different fields, finally resulting in the loop's shape shown in Fig. 2b.

In both cases, the uniaxial character of the substrate's unit cells, (2×4) and (4×6) for InP(0 0 1) and GaAs(0 0 1), respectively, seems to be responsible for the magnetic anisotropy we found. The clearly defined easy- and hard-axis along [$\bar{1}$ 1 0] and [1 1 0], respectively, in the case of the thinnest films, opens the way to realize electronic devices based on spin-dependent electronic transport.

3.3. Fe/MgO/Fe magneto-tunnel junction structures on GaAs(0 0 1)

To achieve the growth of a single crystalline magneto-tunnel junction, we use MgO as the intended tunneling barrier. Recently, local tunneling was observed in the Au/Fe/MgO multilayer grown on an Fe(0 0 1) whisker by scanning probe technique [16]. In the work presented here, a 15 ML thick MgO film was grown epitaxially on 14 ML of Fe previously deposited on InP(0 0 1) and GaAs(0 0 1), without any buffer layer in between. We approached several modes of MgO preparation, as follows: (1) Mg e-beam evaporation in an oxygen atmosphere (not shown), (2) MgO e-beam evaporation and (3) MgO e-beam evaporation in a supporting oxygen atmosphere. Our best results were obtained by evaporating MgO in oxygen atmosphere, and subsequently keeping the sample in about 1×10^{-6} mbar oxygen atmosphere for 12 h. The observed LEED patterns exhibiting a fourfold symmetry confirm a good crystallographic order in the MgO film. After the preparation and characterization of the MgO film, a second 20 ML thick Fe layer was deposited at RT, whose LEED pattern was of lower quality. Eventually, in order to protect the Fe/MgO/Fe structure against oxidation, the samples were covered with about 30 ML of Au, and LEED patterns corresponding to a (5×1) reconstruction of Au(0 0 1) were observed. We repeated exactly the same procedure for the growth of the Au/Fe/MgO/Fe magneto-tunnel structure on InP(0 0 1). However, no LEED patterns were seen after the growth of any layer of the M/FM/I/FM structure. In our opinion, this is caused by a structural disorder at the surface of

the bottom Fe film. This disordered layer might affect the epitaxial growth of the further films building up the junction.

A cross-section of the resulting Au/Fe/MgO/Fe/GaAs(0 0 1) structure, as visible with high-resolution transmission electron microscopy (TEM), is shown in Fig. 3. The images of almost atomic resolution obtained confirm a good crystallographic order in the first Fe and MgO films as well as in the Au cover layer. The interfaces are found to be rather sharp, with a roughness that does not exceed 4 ML at the TEM image scale. Recently it was shown that an FeO layer forms at the Fe/MgO interface [17]. It is worth emphasizing that the MgO film on the scale of TEM images appears continuous and pinhole free. Thus, both Fe films are expected to be electrically insulated, at least at the scale of Fig. 3.

Concerning the top Fe film, which was deposited on the separating MgO layer, the observation of the fourfold in-plane magnetic anisotropy typical for bcc-Fe is expected, with its hard-axis oriented along [1 1 0] and easy-axis along [1 0 0] directions. However, its [1 1 0] axis is easier in comparison to the same axis for the bottom Fe film (e.g. deposited on GaAs(0 0 1)). As shown in Fig. 4a, the contribution of the top Fe film, seen as the low coercivity loop, is clearly visible, whereas that corresponding to the bottom layer is less pronounced due to the more complicated magnetization process described above (Fig. 2b and Section 3.2). Along the [$\bar{1}$ 1 0] direction, which is

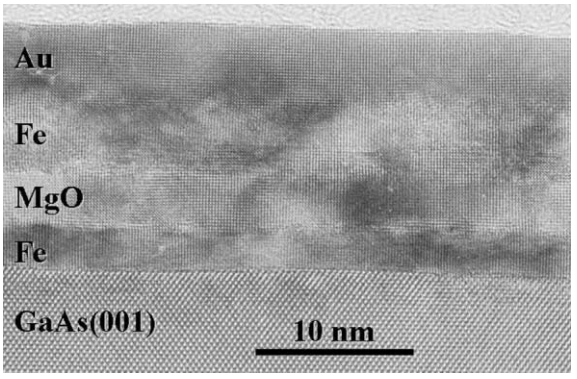

Fig. 3. TEM image over the cross-section of the 30 ML Au/20 ML Fe/15 ML MgO/14 ML Fe/magneto-tunnel junction grown on GaAs(0 0 1).

the easy-axis of magnetization for the Fe film grown on both InP(0 0 1) and GaAs(0 0 1), the coercive field of the bottom Fe film is expected to differ also from the coercivity of the top Fe film. This is confirmed by the typical two-step hysteresis loops measured for the Fe/MgO/Fe/GaAs(0 0 1) structure along the [$\bar{1}$ 1 0]. However, the coercivity in both films differs in this case only slightly (Fig. 4b). For a better definition of the coercive fields in the two Fe films, the top one was made harder by reducing its thickness down to 6 ML and adding about 20 ML of Ni. The thickness of Fe and Ni layers contributing to the top FM film was chosen with respect to the thickness of the bottom Fe film in order to get a nearly zero net magnetization after the first magnetization reversal process (i.e. for antiparallel aligment of magnetization in both FM films). The resulting MOKE loop with two characteristic magnetization jumps is shown in Fig. 4c. By comparison with the MOKE loop of a single Fe layer measured along its easy-axis and showing only one jump (Fig. 2a), one can conclude that each jump is related to the switching of one of the two FM layers. In addition, the net magnetization close to zero clearly confirms that the steps in the MOKE loop correspond to the magnetization reversal processes that occur independently in both FM films (any change of Fe thickness in the top Ni/Fe ferromagnetic film results in a change of the net magnetization of the sample). The loop points at a remarkably increased coercivity in the top layer. This is due to the anisotropy of the Ni/Fe layer which changes as a result of the bcc–fcc phase transition of Ni grown on bcc-Fe(0 0 1) in excess of a critical thickness of about 8 ML, as found by Heinrich et al. [18]. Therefore, the parallel and antiparallel orientations of magnetization in the FM layers, i.e., the independent switching, necessary for a TMR device is achievable in a wide range of the externally applied field.

In order to measure the magnetoresistance, the active area of the junctions selected for further analysis was reduced either by the deposition of the top FM and Au cap layer through a mask (holes diameter of 100 μm) or by a lithographic technique (10 μm × 10 μm). The electrical and magnetic properties of such artificially patterned structures are under investigation.

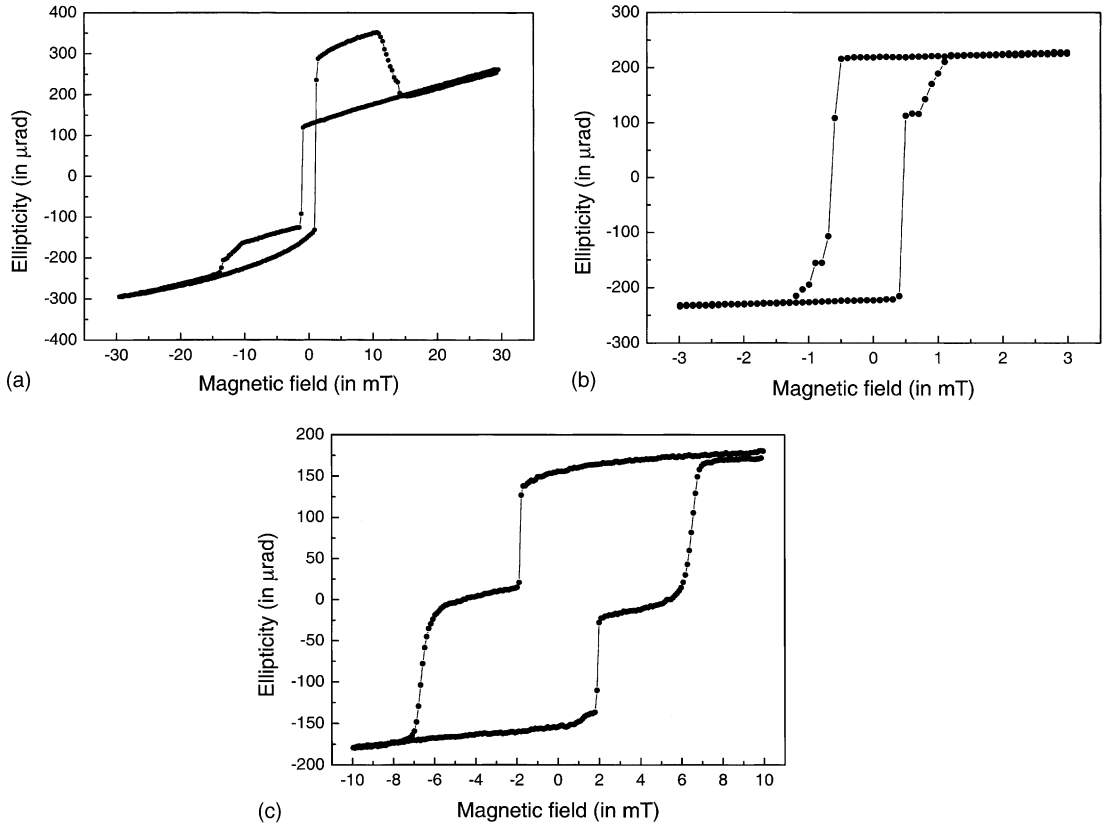

Fig. 4. MOKE loops measured at RT for 20 ML Fe/15 ML MgO/14 ML Fe/GaAs(0 0 1): along (a) [1 1 0] and (b) [$\bar{1}$ 1 0]. A typical two-step hysteresis loop measured for 20 ML Ni/6 ML Fe/10 ML MgO/12 ML Fe/GaAs(0 0 1) along [$\bar{1}$ 1 0] direction is shown in (c).

4. Conclusions

The epitaxial growth of a MgO insulating layer on a thin Fe film previously deposited on GaAs(0 0 1) was successfully realized. A second (top) FM film grown under the same conditions on the MgO layer was proven to be switched individually by an applied magnetic field. The resulting multilayer obtained here can be used to create ballistic spin-polarized electrons by the spin filter effect. Our experimental findings point at a good crystallographic order in the multilayers. In addition, because almost identical electronic states (due to the similar structure and chemical composition of the FM electrodes at the FM/I/FM interfaces) would contribute to tunneling, the junctions we prepared are close to the model one, suitable for comparison with the existing theoretical calculations [10]. On the other hand, its growth directly on GaAs(0 0 1) allows injecting hot electrons by tunneling through the MgO barrier and filtered out in the bottom FM layer into the semiconducting substrate. Due to the spin-filtering effect in the bottom Fe film, the spin polarization of the injected electrons is expected to be remarkably improved.

References

[1] G.A. Prinz, Phys. Today 48 (4) (1995) 58.
[2] R. Fiederling, M. Keim, G. Reuscher, W. Ossau, G. Schmidt, A. Waag, L.W. Molenkamp, Nature 402 (1999) 787.
[3] H.J. Zhu, M. Ramsteiner, H. Kostial, M. Wassermeier, H.-P. Schonherr, K.H. Ploog, Phys. Rev. Lett. 87 (2001) 016601.

[4] G. Schmidt, D. Ferrand, L.W. Molenkamp, A.T. Filip, B.J. van Wess, Phys. Rev. B 62 (2000) R4790.
[5] C.-M. Hu, T. Matsuyama, Phys. Rev. Lett. 87 (2001) 066803.
[6] E.I. Rashba, Phys. Rev. B 62 (2000) R16267.
[7] G. Kirczenow, Phys. Rev. B 63 (2001) 054422.
[8] D.J. Monsma, S.S. Parkin, Appl. Phys. Lett. 77 (2000) 720.
[9] J.S. Moodera, G. Mathon, J. Magn. Magn. Mater. 200 (1999) 248, and references therein.
[10] W.H. Butler, X.-G. Zhang, T.C. Schulthess, J.M. MacLaren, Phys. Rev. B 63 (2001) 054416.
[11] M. Bowen, V. Cros, F. Petroff, A. Fert, C. Martinez Boubeta, J. L. Costa-Krämer, J. V. Anguita, A. Cebollada, F. Briones, J. M. de Teresa, L. Morellón, M.R. Ibarra, F. Güell, F. Peiró, A. Cornet, Appl. Phys. Lett. 79 (2001) 1655.
[12] F. Zavaliche, W. Wulfhekel, J. Kirschner, Phys. Rev. B, submitted for publication.
[13] M. Przybylski, S. Chakraborty, J. Kirschner, J. Magn. Magn. Mater. 234 (2001) 505.
[14] Y.B. Xu, E.T.M. Kernohan, D.J. Freeland, A. Ercole, M. Tselepi, J.A.C. Bland, Phys. Rev. B 58 (1998) 890.
[15] J.M. Florczak, E. Dan Dahlberg, Phys. Rev. B 44 (1991) 9338.
[16] W. Wulfhekel, M. Klaua, D. Ullmann, F. Zavaliche, J. Kirschner, R. Urban, T. Monchesky, B. Heinrich, Appl. Phys. Lett. 78 (2001) 509;
M. Klaua, D. Ullmann, J. Barthel, W. Wulfhekel, J. Kirschner, R. Urban, T.L. Monchesky, A. Enders, J.F. Cochran, B. Heinrich, Phys. Rev. B 64 (2001) 134411.
[17] H.L. Meyerheim, R. Popescu, J. Kirschner, N. Jedrecy, M. Sauvage-Simkin, B. Heinrich, R. Pinchaux, Phys. Rev. Lett. 87 (2001) 076102.
[18] B. Heinrich, Z. Celinski, H. Konno, A.S. Arrott, M. Ruhrig, A. Hubert, Mat. Res. Soc. Symp. Proc. 313 (1993) 485.